Thermal desorption of structured water layer on epitaxial graphene

Cite as: AIP Advances 11, 125012 (2021); doi: 10.1063/5.0075191
Submitted: 19 October 2021 • Accepted: 22 November 2021 •
Published Online: 9 December 2021

Tomoki Minami,[1,a)] Shuta Ochi,[1] Hiroki Nakai,[1] Tomohiro Kinoshita,[1] Yasuhide Ohno,[2] and Masao Nagase[2]

AFFILIATIONS

[1] Graduate School of Advanced Technology and Science, Tokushima University, 2-1 Minamijyousanjima, Tokushima 770-8506, Japan
[2] Institute of Post LED Photonics, Tokushima University, 2-1 Minamijyousanjima, Tokushima 770-8506, Japan

[a)] **Author to whom correspondence should be addressed:** t_minami@ee.tokushima-u.ac.jp

ABSTRACT

Thermal desorption of the structured water layer on graphene was observed in this study via electrical conductivity measurements. Specifically, a structured water layer was formed on the graphene surface via deionized water treatment, following which we examined the thermal desorption process of the layer using sheet resistance measurements. The water molecules acting as a *p*-type dopant were strongly adsorbed on graphene, forming a solid layer. Consequently, the layer was completely removed from the graphene surface at 300 °C. The thermal desorption spectrum of the structured water layer on graphene was quantitatively obtained by converting the measured sheet resistance to carrier density change.

Graphene, a two-dimensional carbon nanomaterial, has excellent properties, such as high electrical mobility and a high surface–volume ratio. Therefore, this material is expected to be applied to various electronic devices.[1–3] In particular, its conductive and stable surface properties, owing to its two-dimensional nature, are expected to be exploited for applications in highly sensitive gas sensors[4–13] and biosensor devices.[14–16] As gas molecules physically adsorb on the graphene surface and directly interact with the π-electron system, the adsorbed molecules act as dopants,[4–13] changing the graphene carrier density. Numerous results on graphene gas sensors have been reported for various gas species and a wide range of concentrations.[4–13] Graphene gas sensors are promising for use in environmental pollutant sensing because of their high sensitivity. For example, nitrogen dioxide (NO_2), whose environmental standard concentration is 40 ppb, can be easily detected.[5–7] In previous reports, the sensitivities of graphene sensors for various gases were seen to be inconsistent with each other because of their initial properties, such as doping concentration, defect, and surface contamination. Furthermore, the graphene channel resistance or conductance change by adsorption or desorption of gas molecules does not provide any information regarding gas species. A gas sensing method with selectivity and quantitative sensitivity for adsorbed gas molecules is therefore required. To solve this problem, we propose thermal desorption spectroscopy (TDS) based on the sheet resistance change of graphene by heating. The TDS or temperature programmable desorption method is known as a conventional method for identifying the adsorbed gas molecules.[17–20] The conventional TDS method uses the mass number information of desorbed molecules measured using a quadrupole mass analyzer and a desorption rate temperature dependence fingerprint to identify the molecular species. In this study, we attempt to implement the conventional TDS concept to the TDS of graphene sheet resistance. The results must be compared with the conventional TDS to verify the concept of the electrical TDS. As reported in several papers, almost all gas molecules are easily desorbed from graphene surfaces in vacuum. For example, water molecules desorb from CVD graphene at ~130 K in vacuum.[21–23] Moreover, previous studies reported that a structured water layer on epitaxial graphene formed by deionized (DI) water treatment was stable in vacuum at room temperature. The solid water layer that was observed by scanning probe microscopy acted as a strong *p*-type dopant for epitaxial graphene on the SiC substrate and was removed by N_2 annealing at 300 °C.[4] Thus, measuring the resistance change by the thermal desorption of structured water on epitaxial graphene could be expected. Furthermore,

the conventional TDS was also measurable. A clear graphene surface water desorption fingerprint was successfully observed in carrier concentration change per rising temperature. The desorption fingerprint was similar to be that of the conventional TDS.

Here, epitaxial graphene was fabricated on a 4H-SiC(0001) semi-insulating substrate by thermal SiC desorption. The sample size was 100 mm^2, and the sample was diced using stealth dicing technology. The SiC substrate was annealed at 1575 °C for 5 min in Ar at 100 Torr for single-layer graphene delineation.[24] Two graphene sample types were prepared. One was a clean graphene sample (annealed) subjected to annealing in dry N_2 at 300 °C after deionized (DI) water cleaning. The surface adsorbent causing the doping was completely removed by annealing up to 300 °C (see Fig. S1 in the supplementary material). The other was with a structured water layer (with water). The structured water layer on epitaxial graphene was formed by immersion in DI water at 23 °C for 60 min. Previous studies have reported that the thickness of the structured water layer is ~0.5 nm, and it acts as a *p*-type dopant against graphene on SiC.[4,25] The desorption process was evaluated loading the sample in a small chamber with an N_2 gas inlet, as shown in Fig. 1. The AlN ceramic heater was placed under the sample for heating to 400 °C. Four electrodes were attached to each corner of the square sample to measure the sheet resistance using the van der Pauw method,[26] and the heater temperature was monitored using a K-type thermocouple. The graphene sheet resistance was measured at a 1 s interval at a constant rising temperature rate of 0.25 °C/s in ambient N_2.

Figure 2 shows the temperature dependences of sheet resistance for two samples, annealed and with water. The sheet resistance of the annealed sample increased monotonically with the rising temperature. The initial sheet resistance at room temperature was 598 Ω/sq. The average temperature coefficient of epitaxial graphene was estimated to be 4.1×10^{-3} for a temperature range from 23 to 300 °C. The temperature dependence of sheet resistance should be attributed to the temperature dependence of mobility as predicted using Matthiessen's law. There are numerous reports on a strong mobility decrease owing to the temperature rising in the approximate room temperature range.[27–29] Conversely, the carrier density of graphene on a semi-insulating substrate had a constant value up to and including 300 K.[30] Furthermore, a mobility temperature factor of β[27–29] giving $\mu(T) = \mu_0(T_0/T)^\beta$, where μ_0 and μ are graphene mobilities at 23 and 300 °C, respectively, can be estimated as 2.66, which is consistent with the previously reported values[27–29] (see Table S1 in the supplementary material). Therefore, the fundamental cause of the sheet resistance change of the annealed sample was the temperature dependence of mobility rather than that of the carrier density. The sheet resistance of graphene with the structured water layer (with water) was 1288 Ω/sq at 23 °C. Because graphene on the SiC substrate is of intrinsically *n*-type doped by the charge transfer between the SiC interface and graphene layers,[31–33] the cause of the increasing sheet resistance of DI water treated graphene is *p*-type doping from the structured water layer on the graphene.[4,25] The difference between the two curves shown in Fig. 2 originates from the doping amount due to the structured water layer. In particular, the graphene conductivity was used to derive the doping amount. The conductivity for both samples is expressed as

$$\sigma_A(T) = en_A(T)\mu_A(T), \tag{1}$$

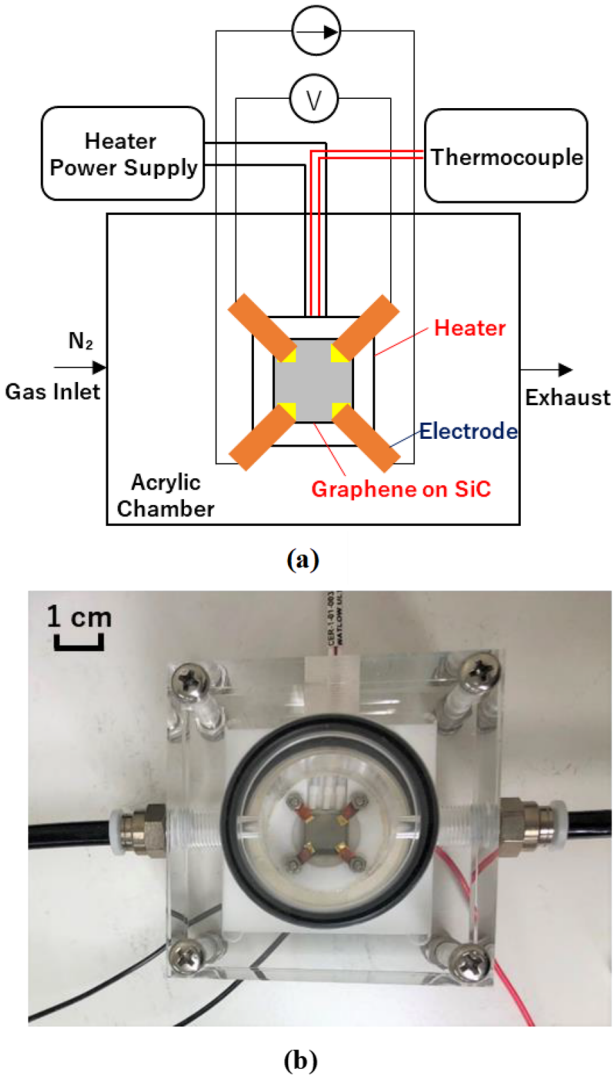

FIG. 1. Thermal desorption measurement system using epitaxial graphene on a SiC substrate. (a) Schematic and (b) photograph of the system. The 100 mm^2 graphene sample was set on an AlN heater with a thermocouple in the environmental control chamber. The sample was fixed using four electrodes to measure the sheet resistance by the van der Pauw method.

$$\sigma_W(T) = en_W(T)\mu_W(T), \tag{2}$$

where σ_A, n_A, and μ_A are the conductivity, sheet carrier density, and mobility of the annealed sample, respectively. σ_W, n_W, and μ_W are the conductivity, sheet carrier density, and mobility of the sample with the water layer, respectively. e is the elemental charge. If n_A is constant for temperature and the temperature dependency of mobility for both samples, $\mu_A(T)$ and $\mu_W(T)$, is the same, the doping amount originating from the structured water layer, $\Delta n(T)$, can be expressed as follows:

$$\Delta n(T) = n_W(T) - n_A = \left(\frac{\sigma_W(T)}{\sigma_A(T)} - 1\right)n_A. \tag{3}$$

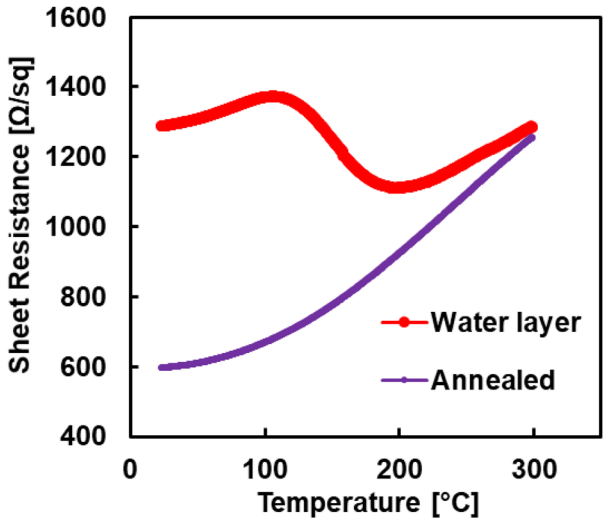

FIG. 2. Temperature dependence of the sheet resistance of graphene on SiC. The red line represents the graphene with a structured water layer (with water), while the blue line represents the annealed graphene (annealed).

Figure 3 shows the temperature dependence of the doping amount, $\Delta n(T)$. At room temperature, the structured water layer doping for epitaxial graphene was ~6.6 × 10^{12} cm^{-2} and of *p*-type. The doping amount was monotonically reduced by the rising temperature due to water desorption. At 170 °C, half of the structured water layer was desorbed. When the sample temperature reached 300 °C, the structured water layer was nearly removed from the graphene surface. This result suggests that the structured water layer is stable at room temperature in dry nitrogen ambient compared with normally adsorbed water molecules[22] and is strongly adsorbed for the graphene surface at over 100 °C, which is the boiling temperature of water. By differentiation of the temperature dependence of the doping amount in Fig. 3, the temperature dependence of the structured water layer desorption rate was estimated, as shown in Fig. 4(a). The desorption rate temperature dependence is maximized at 150 °C. This figure shows a weak peak around 250 °C. The result suggests that there are two desorption processes for strongly adsorbed water on epitaxial graphene. The conventional method for the desorption process measurement with material definition is TDS. Figure 4(b)

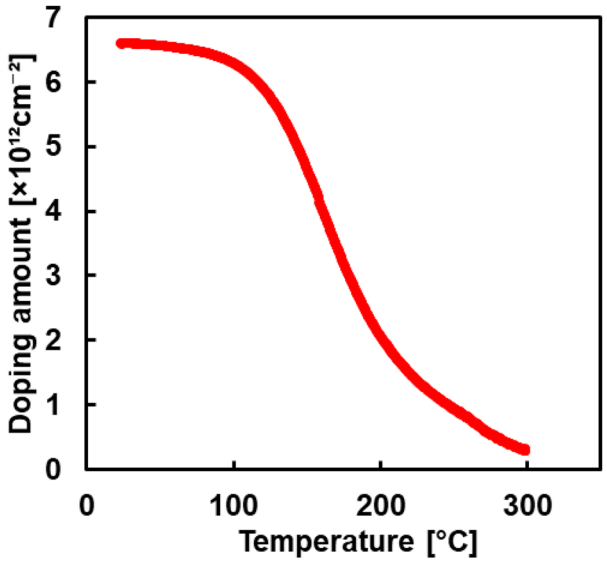

FIG. 3. Temperature dependence of the doping amount, $\Delta n(T)$, originated from the structured water layer.

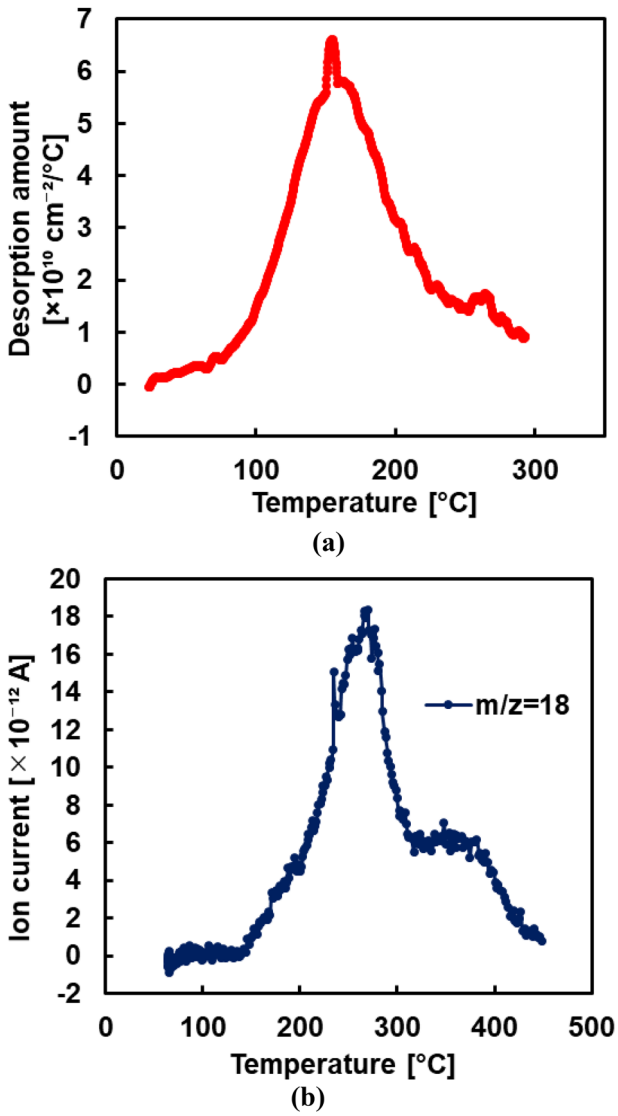

FIG. 4. Thermal desorption spectra of the structured water layer obtained using (a) the graphene sheet resistance measured by the van der Pauw method and (b) conventional TDS of water molecules (m/z = 18) measured using a quadrupole mass spectrometer.

shows the TDS result of water molecules (m/z = 18) from DI water treated graphene on SiC. Two desorption peaks are clearly observed at ~270 and 360 °C. The main peak desorption rate is three times that of the sub-peak. These water desorption process fingerprints, shown in Fig. 4(b), coincide with the desorption rate estimated from sheet resistance change shown in Fig. 4(a). The temperature value cannot be identical for each system because the sample surface temperature is different from the stage thermocouple temperature. Generally, the sample surface temperature value in vacuum should be remarkably lower than that of the stage because of insufficient thermal contact. Alternatively, the sample temperature in atmospheric pressure was expected to be approximately the same as the stage temperature, as shown in Fig. S2. Nevertheless, the TDS of the structured water layer on epitaxial graphene was successfully performed by electronically measuring the sheet resistance. This simple TDS method could be adaptable for environmental sensor devices. Previous studies on graphene gas sensors focused on changes in electrical properties due to gas molecule adsorption to graphene. Thus, they did not focus on the selectivity of the adsorbed gas molecules. There are a few reports concerning sample heating, the purpose of which was simply the desorption of gas molecules. The sample temperature is a very important factor for conventional gas sensors because of selectivity and sensitivity. However, we can acquire limited information regarding the amount of adsorbed water molecules at a constant temperature rising rate in the previous discussions. If the desorption fingerprint of various gas species could be measured, a graphene sensor system consisting of a few graphene chips of different temperatures with high selectivity and sensitivity could be constructed.[8] Further experiments for various gas molecules, such as nitrogen dioxide or sulfur dioxide, are important for establishing the environmental monitoring graphene TDS gas sensor system.

In conclusion, the sheet resistance change of epitaxial graphene at a constant temperature rise rate provides information regarding the desorption process of the structured water layer. The temperature dependence of the adsorbed water desorption rate estimated from the carrier density of graphene coincided with the result measured by conventional TDS. The structured water layer on epitaxial graphene was nearly stable below 100 °C. The maximum desorption rate was observed at ~150 °C. The desorption fingerprint will play a crucial role in identifying adsorbed molecules and realizing graphene gas sensors in the future.

See the supplementary material for additional information regarding the change in sheet resistance due to heating.

This work was supported by JSPS KAKENHI Grant Nos. JP19H02582 and JP21H01394.

We would like to acknowledge Editage (www.editage.com) for English language editing.

AUTHOR DECLARATIONS

Conflict of Interest

The authors have no conflicts of interest directly relevant to the content of this article.

Author Contributions

All authors contributed equally to this work.

DATA AVAILABILITY

The data that support the findings of this study are available from the corresponding author upon reasonable request.

REFERENCES

[1] K. S. Novoselov, A. K. Geim, S. V. Morozov, D. Jiang, Y. Zhang, S. V. Dubonos, I. V. Grigorieva, and A. A. Firsov, Science **306**(5696), 666–669 (2004).
[2] K. S. Novoselov, A. K. Geim, S. V. Morozov, D. Jiang, M. I. Katsnelson, I. V. Grigorieva, S. V. Dubonos, and A. A. Firsov, Nature **438**(7065), 197–200 (2005).
[3] C. Lee, X. Wei, J. W. Kysar, and J. Hone, Science **321**(5887), 385–388 (2008).
[4] M. Kitaoka, T. Nagahama, K. Nakamura, T. Aritsuki, K. Takashima, Y. Ohno, and M. Nagase, Jpn. J. Appl. Phys., Part 1 **56**(8), 085102 (2017).
[5] F. Schedin, A. K. Geim, S. V. Morozov, E. W. Hill, P. Blake, M. I. Katsnelson, and K. S. Novoselov, Nat. Mater. **6**(9), 652–655 (2007).
[6] S. Novikov, N. Lebedeva, and A. Satrapinski, J. Sens. **2015**, 108581.
[7] S. Novikov, N. Lebedeva, A. Satrapinski, J. Walden, V. Davydov, and A. Lebedev, Sens. Actuators, B **236**, 1054 (2016).
[8] C. Melios, V. Panchal, K. Edmonds, A. Larrrtsev, R. Yakimova, and O. Kazakova, ACS Sens. **3**, 1666–1674 (2018).
[9] C. W. Chen, S. C. Hung, M. D. Yang, C. W. Yeh, C. H. Wu, G. C. Chi, F. Ren, and S. J. Pearton, Appl. Phys. Lett. **99**, 243502 (2011).
[10] R. Jaaniso, T. Kahro, J. Kozlova, J. Aarik, L. Aarik, H. Alles, A. Floren, A. Gerst, A. Kasikov, A. Niilisk, and V. Sammelselg, Sens. Actuators, B **190**, 1006–1013 (2014).
[11] T. Wang, D. Huang, Z. Yang, S. Xu, G. He, X. Li, N. Hu, G. Yin, D. He, and L. Zhang, Nano-Micro Lett. **8**(2), 95–119 (2016).
[12] H. J. Yoon, D. H. Jun, J. H. Yang, Z. Zhou, S. S. Yang, and M. M.-C. Cheng, Sens. Actuators, B **157**(1), 310–313 (2011).
[13] F. Ricciardella, S. Vollebregt, T. Polichetti, M. Miscuglio, B. Alfano, M. L. Miglietta, E. Massera, G. Di Francia, and P. M. Sarro, Nanoscale **9**(18), 6085–6093 (2017).
[14] G. Seo, G. Lee, M. J. Kim, S.-H. Baek, M. Choi, K. B. Ku, C.-S. Lee, S. Jun, D. Park, H. G. Kim, S.-J. Kim, J.-O. Lee, B. T. Kim, E. C. Park, and S. I. Kim, ACS Nano **14**(4), 5135–5142 (2020).
[15] Y. Ohno, K. Maehashi, Y. Yamashiro, and K. Matsumoto, Nano Lett. **9**(9), 3318–3322 (2009).
[16] Y. Taniguchi, T. Miki, Y. Ohno, M. Nagase, Y. Arakawa, Y. Imada, K. Minagawa, and M. Yasuzawa, Jpn. J. Appl. Phys., Part 1 **58**, 055001 (2019).
[17] R. S. Smith and B. D. Kay, J. Phys. Chem. B **122**(2), 587–594 (2018).
[18] J. P. Meyburg, I. I. Nedrygailov, E. Hasselbrink, and D. Diesing, Rev. Sci. Instrum. **85**(10), 104102 (2014).
[19] S. Abe, H. Handa, R. Takahashi, K. Imaizumi, H. Fukidome, and M. Suemitsu, Jpn. J. Appl. Phys., Part 1 **50**(7R), 070102 (2011).
[20] H. Atsumi, Y. Takemura, T. Konishi, T. Tanabe, and T. Shikama, J. Nucl. Mater. **438**, S963–S966 (2013).
[21] U. Burghaus, Inorganics **4**(2), 10 (2016).
[22] U. Burghaus, J. Mater. Res. **36**, 129 (2020).
[23] A. Chakradhar and U. Burghaus, Chem. Commun. **50**(57), 7698–7701 (2014).
[24] T. Aritsuki, T. Nakashima, K. Kobayashi, Y. Ohno, and M. Nagase, Jpn. J. Appl. Phys., Part 1 **55**, 06GF03 (2016).
[25] J. Du, Y. Kimura, M. Tahara, K. Matsui, H. Teratani, Y. Ohno, and M. Nagase, Jpn. J. Appl. Phys., Part 1 **58**, SDDE01 (2019).
[26] L. J. van der Pauw, Philips Res. Rep. **13**, 174 (1958).

[27]S. Tanabe, Y. Sekine, H. Kageshima, M. Nagase, and H. Hibino, Phys. Rev. B **84**, 115458 (2011).
[28]R.-J. Shiue, Y. Gao, C. Tan, C. Peng, J. Zheng, D. K. Efetov, Y. D. Kim, J. Hone, and D. Englund, Nat. Commun. **10**(1), 109 (2019).
[29]V. E. Dorgan, M.-H. Bae, and E. Pop, Appl. Phys. Lett. **97**(8), 082112 (2010).
[30]A. J. M. Giesbers, P. Procházka, and C. F. J. Flipse, Phys. Rev. B **87**(19), 195405 (2013).
[31]F. Varchon, R. Feng, J. Hass, X. Li, B. N. Nguyen, C. Naud, P. Mallet, J.-Y. Veuillen, C. Berger, E. H. Conrad, and L. Magaud, Phys. Rev. Lett. **99**(12), 126805 (2007).
[32]J. Hass, W. A. De Heer, and E. H. Conrad, J. Phys.: Condens. Matter **20**, 323202 (2008).
[33]S. Kopylov, A. Tzalenchuk, S. Kubatkin, and V. I. Fal'ko, Appl. Phys. Lett. **97**(11), 112109 (2010).